J|A|C|S
ARTICLES
Published on Web 01/18/2006

Utilization of the Pleiotropy of a Peptidic Aptamer To Fabricate Heterogeneous Nanodot-Containing Multilayer Nanostructures

Ken-Ichi Sano,[†] Hiroyuki Sasaki,[‡] and Kiyotaka Shiba*,[†]

Contribution from the Department of Protein Engineering, Cancer Institute, Japanese Foundation for Cancer Research and CREST, JST, Koto, Tokyo 135-8550, Japan, and Department of Molecular Cell Biology, Institute of DNA Medicine, The Jikei University School of Medicine, Minato, Tokyo 105-8461, Japan

Received October 24, 2005; E-mail: kshiba@jfcr.or.jp

Abstract: Peptide aptamers (=binders) against inorganic materials often show a capacity for mineralization of their target atoms; thus they are able to function both as binding molecules and as mediators for mineralization. Although the mechanisms underlying these two properties of peptide aptamers are not yet fully understood, they have been used separately to fabricate various nanostructures. Here, we present a novel method of nanofabrication, in which binding and mineralization by a peptide aptamer are alternately utilized to assemble multilayered nanostructures comprised of metal loaded cage proteins ornamented with Ti-binding peptides.

Introduction

One of the most remarkable aspects of biomacromolecules is their ability to recognize a wide array of substances with a high degree of specificity, as exemplified by antibody−antigen interactions.[1] This feature of biomolecules has been extensively explored with the aim of developing new tools in material sciences,[2,3] and a number of artificial peptide aptamers that specifically recognize various inorganic materials have been created by selecting binders from random arrays of amino acids displayed on phages or bacteria.[3−10] We previously used a peptide-phage display system to isolate a peptide aptamer (TBP-1, titanium binding peptide-1) that electrostatically binds to Ti surfaces.[9] Subsequently, we found that TBP-1 also specifically binds to Ag and Si surfaces, but not to Au, Cr, Pt, Sn, Zn, Cu, or Fe under conditions where nonspecific hydrophobic interactions were suppressed.[11] Mutations that diminished the binding of TBP-1 to Ti also diminish its affinity for Ag and Si,[9,11] suggesting TBP-1 recognizes a local electrostatic structure shared among the oxidized surfaces of these three metals.

TBP-1 also possesses the capacity to mediate mineralization. In the presence of TBP-1, nanocrystals 300−500 nm in size were grown from silver nitrate solution.[11] Similarly, silicification from prehydrolyzed tetramethoxysilane (TMOS) was accelerated in the presence of TBP-1 and was suppressed by amino acid substitutions in TBP-1 that also impaired the binding of the mutant peptide to Ti, Ag, and Si.[11] Thus, TBP-1 is bifunctional in that it acts as both a metal-binding peptide and a mediator for mineralization.

TBP-1 comprises 12 amino acids, and its sequence is NH_2-Arg-Lys-Leu-Pro-Asp-Ala-Pro-Gly-Met-His-Thr-Trp-COOH.[9] Mutational analyses have shown that it is the first hexapeptide in the sequence that mediates Ti binding and that the identities of Arg1, Pro4, and Asp5 are critical for such binding.[9] Moreover, this hexapeptide (called minTBP-1) has the ability to endow xenogeneic molecules with specific affinities. For instance, we inserted a DNA fragment encoding minTBP-1 into the 5′ end of the gene encoding the L-chain of horse ferritin, yielding a ferritin-like cage protein, minT1-LF, with a diameter of about 12 nm in *Escherichia coli* that was able to bind to QCM sensors made of Ti or SiO_2, but not to one made of Au, in the presence of 0.05% Tween 20.[12] QCM analyses also showed that minT1-LF possessed stronger affinities for Ti and SiO_2 (K_D = 3.82 nM for Ti and 4.44 nM for SiO_2) than the parental TBP-1 (K_D = 13.2 μM for Ti), affinities comparable to those typically observed with natural biomolecules.[12] This increased affinity almost certainly reflects the multivalency of the protein (ferritin

[†] Japanese Foundation for Cancer Research and CREST.
[‡] The Jikei University School of Medicine.

(1) Amit, A. G.; Mariuzza, R. A.; Phillips, S. E.; Poljak, R. J. *Science* **1986**, *233*, 747−753.
(2) Flynn, C. E.; Lee, S. W.; Peelle, B. R.; Belcher, A. M. *Acta Mater.* **2003**, *51*, 5867−5880.
(3) Sarikaya, M.; Tamerler, C.; Jen, A. K.; Schulten, K.; Baneyx, F. *Nat. Mater.* **2003**, *2*, 577−585.
(4) Brown, S. *Proc. Natl. Acad. Sci. U.S.A.* **1992**, *89*, 8651−8655.
(5) Kase, D.; Kulp, J. L. I.; Yudasaka, M.; Evans, J. S.; Iijima, S.; Shiba, K. *Langmuir* **2004**, *20*, 8931−8941.
(6) Lee, S. W.; Mao, C.; Flynn, C. E.; Belcher, A. M. *Science* **2002**, *296*, 892−895.
(7) Naik, R. R.; Brott, L. L.; Clarson, S. J.; Stone, M. O. *J. Nanosci. Nanotechnol.* **2002**, *2*, 95−100.
(8) Naik, R. R.; Stringer, S. J.; Agarwal, G.; Jones, S. E.; Stone, M. O. *Nat. Mater.* **2002**, *1*, 169−172.
(9) Sano, K.; Shiba, K. *J. Am. Chem. Soc.* **2003**, *125*, 14234−14235.
(10) Whaley, S. R.; English, D. S.; Hu, E. L.; Barbara, P. F.; Belcher, A. M. *Nature* **2000**, *405*, 665−668.
(11) Sano, K.; Sasaki, H.; Shiba, K. *Langmuir* **2005**, *21*, 3090−3095.
(12) Sano, K.; Ajima, K.; Iwahori, K.; Yudasaka, M.; Iijima, S.; Yamashita, I.; Shiba, K. *Small* **2005**, *1*, 826−832.

10.1021/ja057262r CCC: $33.50

is a polyhedral protein composed of 24 subunits[13]) and the reduced diffusion coefficient of the immobilized minTBP-1.

Polyhedral cage proteins such as virus capsids,[14] lumazine synthase,[15] and heat-shock proteins,[16] as well as ferritin,[17] have been attracting attention as promising building blocks for nanofabrication because they can hold a variety of inorganic materials within their interior spaces. We have already shown that N-terminal engineered recombinant ferritin retains its ability to store oxidized Fe within its inner space, so that a peptide aptamer displaying ferritin could serve as a versatile block for allocating inorganic nanoparticles to specific regions.[12] Here, we show a novel method of nanofabrication, in which binding and mineralization by a peptide aptamer are alternately utilized to assemble multilayered nanostructures composed of metal-loaded peptide aptamers displaying ferritin.

Experimental Section

Ferritin Preparation. Construction, expression, and purification of minT1-LF and Δ1-LF have been described previously.[12] The expression plasmid for minT1(R1A)-LF, in which the first Arg of minTBP-1 was substituted with an Ala, was constructed by inserting a 5′-phosphorylated oligonucleotide duplex (KY-1439, GAT CCA TAT GGC GAA ACT TCC GGA TGC GAG CT; and KY-1440, CGC ATC CGG AAG TTT CGC CAT ATG) into the *Bam*HI and *Sac*I sites of the pKIT0 plasmid.[12] The expression and purification of minT1(R1A)-LF followed the procedures for minT1-LF and Δ1-LF. The molecular weight of the mutated L-chain in the assembled ferritin was determined to be 20435.2 using MALDI-TOF. This value agreed well with the calculated molecular weight of 20426.1 if the first methionine residue was posttranslationally removed in *E. coli*, as was the case for Δ1-LF. The concentrations of the apoferritins were determined spectrophotometrically with a molecular extinction coefficient of 13370 at 280 nm.

The purified apo-minT1-LF particles were filled with Fe, Co, or CdSe as described[12,18,19] to obtain Fe@minT1-LF, Co@minT1-LF, and CdSe@minT1-LF. The concentrations of Fe, Co, and CdSe-filled ferritins were determined using the Bradford method[20] with apo-minT1-LF serving as a calibrator.

Silicification Assay. Silicification was started by mixing prehydrolyzed 0.1 M TMOS (Shinetsu Silicone, Tokyo) in TBS (Tris-buffered saline, 50 mM TrisHCl pH7.5 and 150 mM NaCl) with 0.5 mg/mL minT1-LF or Δ1-LF at ambient temperature. The prehydrolysis was done by incubating 1 M TMOS in 1 mM HCl for 5 min at 25 °C, after which 10 volumes of TBS was added to start the reaction. Formation of silica was monitored by measuring scattered light (λ = 350 nm) at 90° with a JASCO FP-6500.

BioLBL. Multilayered nanostructures were fabricated and monitored on the quartz sensor of a QCM-D300 (Q-sense AB, Göteborg). The sensor had a surface area of approximately 150 mm^2 and was equipped with a measurement cell having a volume of approximately 80 μL. The temperature of the chamber was kept at 25.0 ± 0.05 °C, and QCM data were collected at 14.8 MHz. We used Ti- or Au-coated sensors, both of which were purchased from Q-sense AB. The initial minT1-LF layer was applied to the Ti-sensor by filling the measurement cell with 0.1 mg/mL of apo-minT1-LF or 0.2 mg/mL of metal filled-minT1-LF in TBS. To form the first layer of minT1(R1A)-LF or Δ1-LF, we used an Au-coated sensor. To prepare TEM samples, we used an Au-coated sensor because the Ti-coated sensor fractured during cross sectioning.

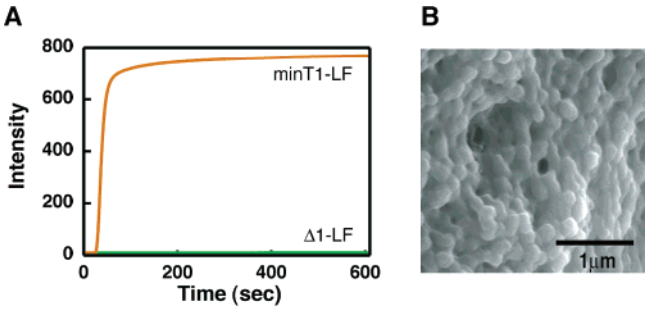

Figure 1. Silicification catalyzed by minT1-LF. (A) Silicification was started at time = 0 by mixing prehydrolyzed 0.1 M TMOS in TBS with 0.5 mg/mL minT1-LF (orange) or Δ1-LF (green). Silica formation was monitored by measuring scattered light (λ = 350 nm, arbitrary units) at 90° with a JASCO FP-6500. (B) SEM image of the silica formed in the presence of minT1-LF. Bar represents 1 μm.

After the first layer of ferritin was formed (judged by changes of resonance frequency of QCM), the sensor was washed with 1.5 mL of TBS and then incubated with 0.1 M prehydrolyzed TMOS in TBS. The silicification process was terminated by flowing 1.5 mL of TBS into the measurement chamber. Formation of the second (and later) ferritin layer was accomplished in the same way as the first.

EM Observations. To make observations using SEM, we fabricated the layers on a mirror-polished Ti substrate (6 mm × 6 mm, JIS I grade, Shinkinzoku-Kougyou, Toyonaka). Before layer formation, the Ti substrates were extensively washed with TBS five times and then incubated for 10 min at room temperature with 1 mL of 0.1 mg/mL Fe@minT1. After the substrates were washed with TBS, the silicification was started by incubating the substrate with 1 mL of 0.1 M prehydrolyzed TMOS in TBS for 10 min. The same procedures were repeated to obtain two alternating layers of Fe@minT1-LF and silica. The surfaces were then coated with gold−palladium using a HITACHI E-1030 ion sputter at 14 mA for 150 s and observed using a Hitachi S-4300 at 5 kV.

An EM-002BF/P-20 (TOPCON, Tokyo) TEM was used at 200 kV to observe cross sections of multilayers. The samples were prepared using the ion-milling method[21] and stained by osmium. EDS analyses were carried out using a NORAN system VI (Thermo Electron Corp., Waltham); the probe radius was 0.7 nm, and the probe current was 500 pA.

Results and Discussion

Silicification Activity of minT1-LF. We began the study described here by confirming that minT1-LF inherited the capacity for silicification exhibited by parental TBP-1. When we incubated minT1-LF with prehydrolyzed TMOS in a test tube, a white precipitate appeared within 1 min. No such precipitation was seen when Δ1-LF, which lacks the minTBP-1 peptide,[12] or minT1(R1A)-LF, in which a critical residue (Arg1) of minTBP-1 was substituted by Ala (see below), was incubated under the same conditions (data not shown). Analysis of light scattering in the solutions confirmed that the precipitate formed (as indicated by an increase in light scattering) within 60 s in the presence of 0.5 mg/mL minT1-LF, but the same concentration of Δ1-LF caused no increase in scattering, even after incubating 10 min (Figure 1A). SEM revealed that the precipitate was made up of spherical particles with diameters of 150−250

(13) Banyard, S. H.; Stammers, D. K.; Harrison, P. M. *Nature* **1978**, *271*, 282−284.
(14) Douglas, T.; Young, M. *Nature* **1998**, *393*, 152−155.
(15) Laplagne, D. A.; Zylberman, V.; Ainciart, N.; Steward, M. W.; Sciutto, E.; Fossati, C. A.; Goldbaum, F. A. *Proteins* **2004**, *57*, 820−828.
(16) McMillan, R. A.; Paavola, C. D.; Howard, J.; Chan, S. L.; Zaluzec, N. J.; Trent, J. D. *Nat. Mater.* **2002**, *1*, 247−252.
(17) Yamashita, I. *Thin Solid Films* **2001**, *393*, 12−18.
(18) Iwahori, K.; Yoshizawa, K.; Muraoka, M.; Yamashita, I. *Inorg. Chem.* **2005**, *44*, 6393−6400.
(19) Tsukamoto, R.; Iwahori, K.; Muraoka, M.; Yamashita, I. *Bull. Chem. Soc. Jpn.* **2005**, *78*, 2075−2081.
(20) Bradford, M. M. *Anal. Biochem.* **1976**, *72*, 248−254.
(21) Abrahams, M. S.; Buiocchi, C. J. *J. Appl. Phys.* **1974**, *45*, 3315−3316.

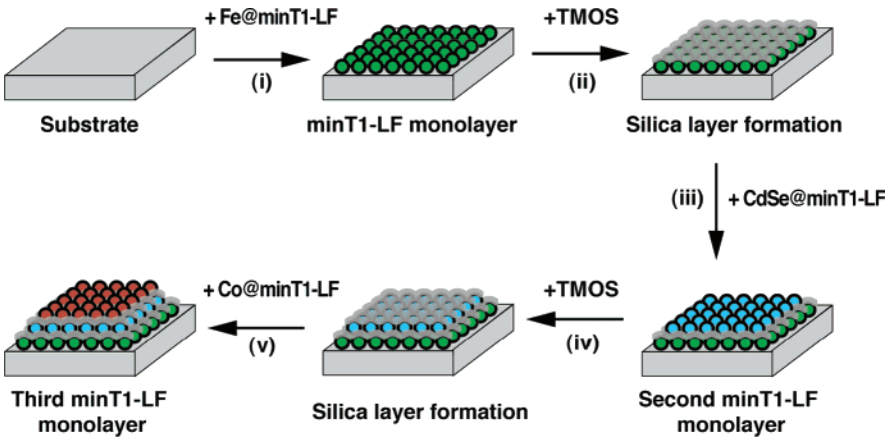

Figure 2. Schematic representation of BioLBL. The first monolayer of minT1-LF is formed by the interaction between minTBP-1 and Ti (i). On top of the layer of the minT1-LF, a silica layer is deposited via mineralization mediated by minTBP-1 (ii). The second monolayer of minT1-LF is deposited through the interaction between minTBP-1 and silica (iii). The next silica layer is deposited on the second minT1-LF layer (iv), after which the third minT1-LF layer is deposited (v). By using different types of minT1-LF containing different metal compounds (Fe@minT1-LF, CdSe@minT1-LF, and Co@minT1-LF), heterogeneous multilayer nanostructures are constructed (i, iii, v).

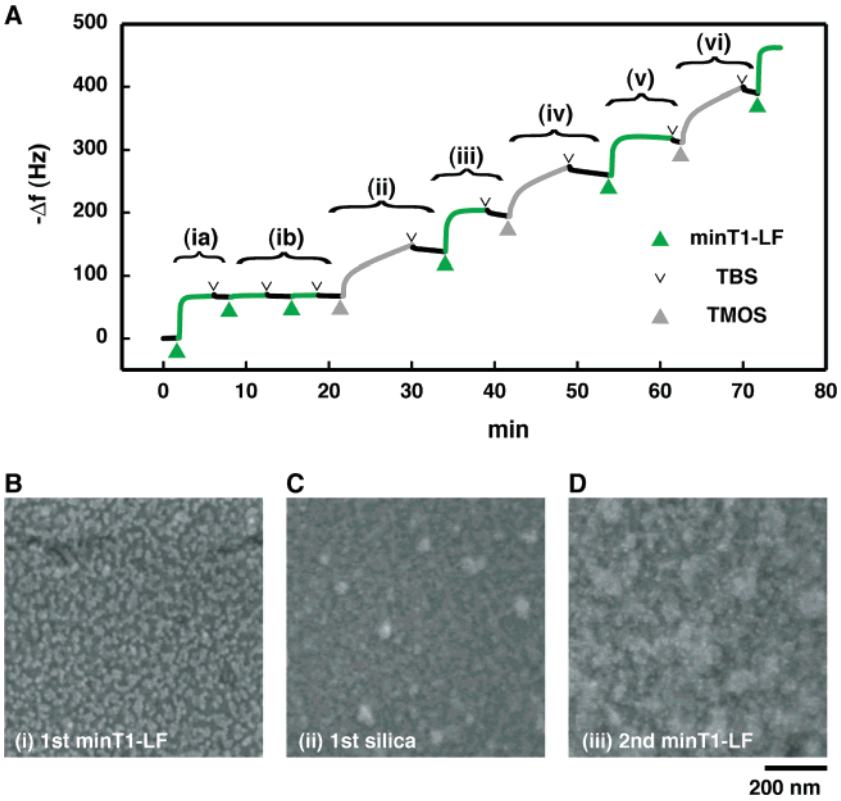

Figure 3. Characterization of multilayer structures fabricated by BioLBL. (A) Time-dependent changes in resonance frequency (*f*) during QCM analysis. Note that the values on the longitudinal axis represent the negative of Δ*f*. Changes associated with adsorption of minT1-LF and silicification are shown by green and gray lines, respectively. Green and gray arrowheads represent the respective time points at which minT1-LF and TMOS were infused into the measurement chamber. V's represent the respective time points at which wash solution (TBS) was infused. See text for (ia)−(vi). (B−D) Surfaces of the intermediates as observed by SEM. A first ferritin layer (B), the following silica layer (C), and the second ferritin layer (D) are shown. In this experiment, Fe@minT1-LF was used to provide high contrast for the micrograph.

nm (Figure 1B), while EDS mapping showed both Si and O to be present (data not shown). Thus, addition of minTBP-1 endowed ferritin with the silicification and binding characteristics of TBP-1.

BioLBL. By taking advantage of the bifunctionality of minT1-LF, we have been able to design a novel method for the assembly of multilayered nanostructures, which we call BioLBL (biomimetic layer-by-layer assembly). The BioLBL scheme is illustrated (Figure 2). First, a solid titanous substrate is covered with a monolayer of minT1-LF; this is achieved via the specific binding of minTBP-1 to the Ti [Figure 2(i)]. Twenty-four minTBP-1 molecules are near-symmetrically distributed on the surface of each ferritin molecule,[12] some of which are not engaged in Ti binding or interaction with the adjoining ferritin molecule and are thus free to access chemical compounds in the solution. Consequently, addition of prehydrolyzed TMOS results in the deposition of a silica film on the layered ferritins by virtue of silicification mediated by minT1-LF [Figure 2(ii)]. The newly formed silica film is then the binding target of minT1-LF, and a second minT1-LF monolayer is formed on

the silica [Figure 2(iii)]. This second layer of minT1-LF can then serve as catalyst for a second deposition of silica film [Figure 2(iv)], which in turn serves as the target for a third minT1-LF layer [Figure 2(v)]. This cycle of minT1-LF binding and silicification can be repeated until the desired number of layers is reached. Because many types of metal compounds can be encapsulated within the interior space of ferritin,[18,22−27] our BioLBL method should enable ferritin containing a variety of nanodots to be layered in a programmable manner.

We tested the feasibility of this new method using QCM by monitoring changes in the resonance frequency (f) of a Ti sensor treated as described in Figure 2. Initial infusion of minT1-LF solution into the QCM measurement cell immediately reduced the resonance frequency of the sensor by approximately 65 Hz; this response plateaued within 1 min and was little affected by subsequent infusion of a wash buffer, indicating that minT1-LF was tightly bound to the Ti surfaces [Figure 3A(ia); note that the longitudinal axis represents negative values of Δf]. The idea that the adsorbed minT1-LF formed a monolayer on the Ti substrate is supported by the following calculation: the 65 Hz reduction in resonance frequency corresponds to an increase in weight of 1.1 μg/cm^2 on the tip (when the viscoelasticity of adsorbed molecule was neglected), which agrees fairly well with the weight of 0.9 μg/cm^2 calculated by multiplying the number of minT1-LF molecules adsorbed (4.8×10^{11} /cm^2, estimated by SEM; data not shown) by the weight of a liquid-phase apoferritin molecule (1.8×10^{-12} μg).[28] Furthermore, two additional infusions of minT1-LF followed by a wash did not change the resonance frequency of the sensor, indicating the multiple layers of minT1-LF cannot be formed under these conditions [Figure 3A(ib)]. After the first minT1-LF monolayer was deposited, we infused a solution containing prehydrolyzed TMOS, which elicited a gradual decline in resonance frequency that was preceded by an initial rapid decrease, reflecting the layer of silica deposited via minT1-LF-mediated mineralization [Figure 3A(ii)]. We continued the silicification reaction for approximately 9 min, after which it was stopped by washing out the TMOS solution with TBS. When the cell chamber was refilled with minT1-LF solution, the resonance frequency again declined by 65 Hz, indicating the deposition of a second ferritin monolayer on top of the silica layer [Figure 3A(iii)]. The two successive cycles of TMOS and minT1-LF treatments (iv−vii) gave essentially the same pattern of change in resonance frequency, indicating the stepwise deposition of layers on the QCM sensor. Within the minT1-LF layers, small particles corresponding to ferritin were visible with SEM, whereas no particles were observed on the silica layers (Figure 3B−D).

To confirm the importance of the minTBP-1 peptide sequence to the BioLBL process, we conducted similar experiments with Δ1-LF ferritin (recombinant wild-type horse L-ferritin) and minT1(R1A)-LF (which displays a mutant aptamer incapable of binding or silicification). In these experiments, we deposited the first ferritin layer by making use of a nonspecific interaction between the sensor substrate and ferritin molecules because Δ1-LF and minT1(R1A)-LF have no specific affinity to Ti. We therefore used a QCM sensor coated with Au that was able to nonspecifically adsorb proteins via hydrophobic interactions.[28] We previously showed that a minT1-LF did not bind to Au when the hydrophobic surface of the sensor was masked by 0.05% Tween 20.[12] In the absence of those blocking reagents, ferritin irreversibly bound to Au via hydrophobic interactions (data not shown). After the nonspecific binding of the first layer of ferritin to the sensor, we were able to fabricate multilayer structures composed of silica and ferritin using minT1-LF as the ferritin source (Figure 4A). When we used Δ1-LF instead

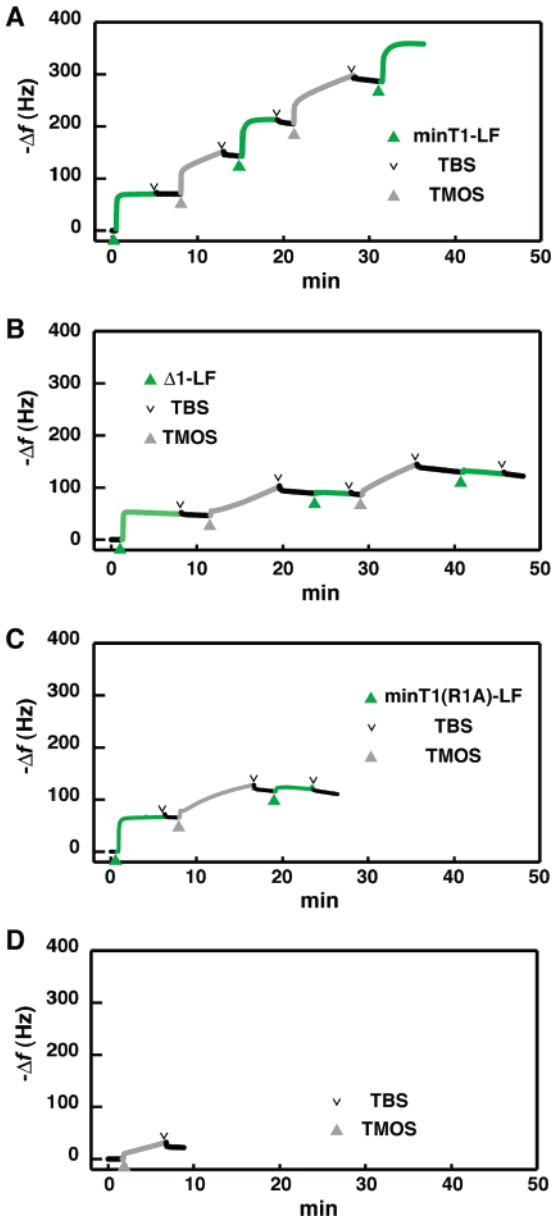

Figure 4. Time-dependent changes in resonance frequency (f) during QCM. (A) Layers of minT1-LF were deposited on an Au-coated sensor with intervening silica layers. Note that the values on the longitudinal axis represent the negative of Δf. Changes associated with adsorption of minT1-LF and silicification are shown by green and gray lines, respectively. Green and gray arrowheads represent the respective time points at which minT1-LF and TMOS were infused into the measurement chamber. V's represent the respective time points at which wash solution (TBS) was infused. (B) Δ1-LF was used instead of minT1-LF. (C) The mutant minT1(R1A)-LF was used as in (C). (D) Basal level of silicification on an Au-coated sensor.

(22) Douglas, T.; Stark, V. T. *Inorg. Chem.* **2000**, *39*, 1828−1830.
(23) Hainfeld, J. F. *Proc. Natl. Acad. Sci. U.S.A.* **1992**, *89*, 11064−11068.
(24) Mann, S.; Bannister, J. V.; Williams, R. J. *J. Mol. Biol.* **1986**, *188*, 225−232.
(25) Okuda, M.; Kobayashi, Y.; Suzuki, K.; Sonoda, K.; Kondoh, T.; Wagawa, A.; Kondo, A.; Yoshimura, H. *Nano Lett.* **2005**, *5*, 991−993.
(26) Wong, K. K. W.; Mann, S. *Adv. Mater.* **1996**, *8*, 928−932.
(27) Yamashita, I.; Hayashi, J.; Hara, M. *Chem. Lett.* **2004**, *33*, 1158−1159.
(28) Höök, F.; Rodahl, M.; Brzezinski, P.; Kasemo, B. *J. Colloid Interface Sci.* **1998**, *208*, 63−67.

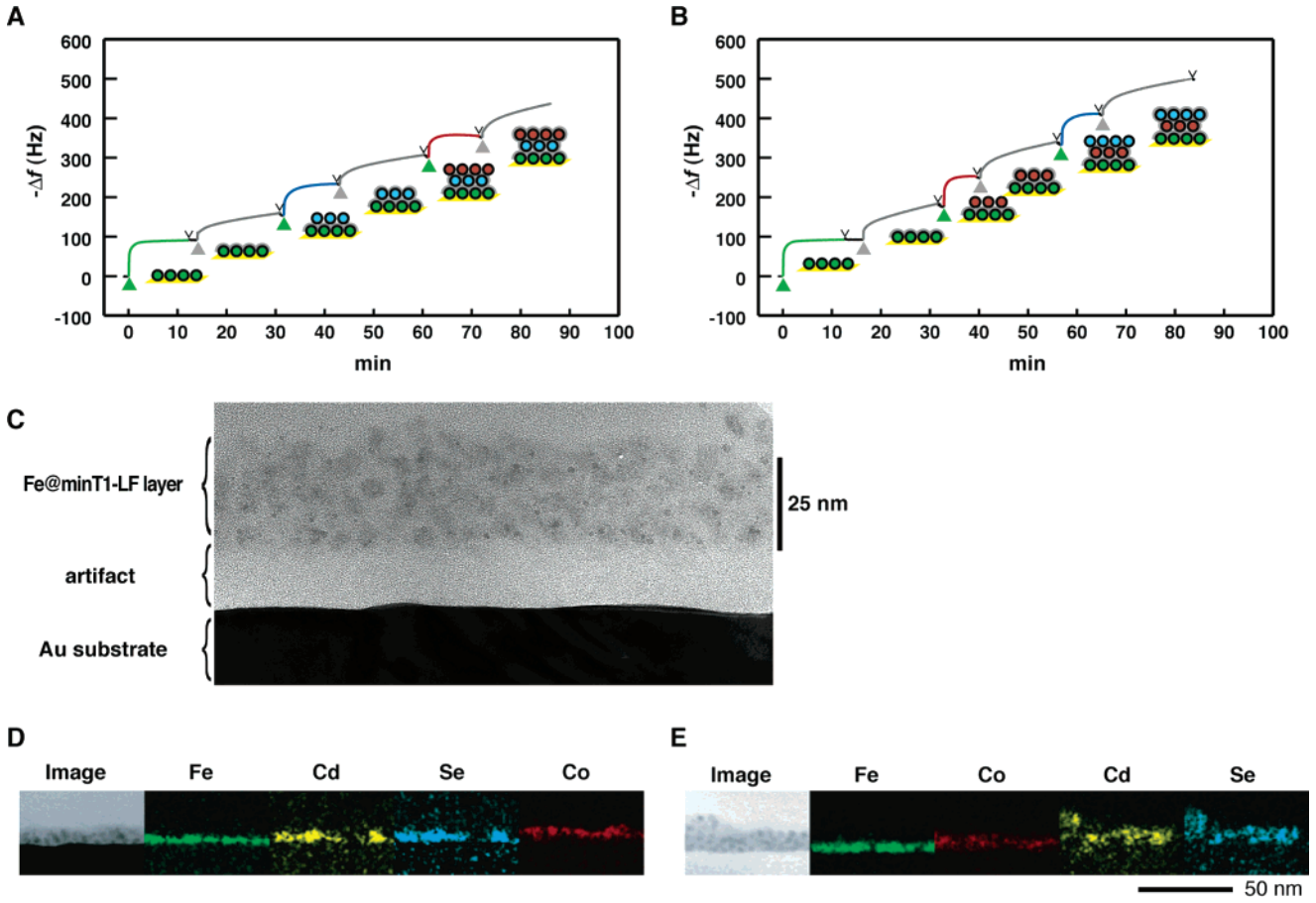

Figure 5. Fabrication of heterogeneous multilayer structures using metal-loaded minT1-LF. (A) Time-dependent changes in resonance frequency (*f*) during QCM analysis of the fabrication of heterogeneous multilayer structures. In this experiment, Fe@minT1-LF, CdSe@minT1-LF, and Co@minT1-LF were layered on an Au-coated sensor in that order with intervening silica layers. See Figure 2 legend for details. (B) Same as (A), but the order was changed to Fe@minT1-LF, Co@minT1-LF, and CdSe@minT1-LF. (C) TEM image of the cross-section of a multilayer structure having three Fe@minT1-LF layers. The space between the Ti substrate and the minT1-LF layer is believed to be an artifact introduced during preparation of the sample. (D) EDS mapping of a cross-section of the Fe@minT1-LF, CdSe@minT1-LF, and Co@minT1-LF layers. (E) EDS mapping of a cross-section of the Fe@minT1-LF, Co@minT1-LF, and CdSe@minT1-LF layers.

of minT1-LF, however, deposition of the first silica layer proceeded at a very slow rate that was comparable to the rate observed with silicification of Au (Figure 4B and D). Furthermore, we were unable to apply the second Δ1-LF layer to the silica layer (Figure 4B). Similar results were obtained with minT1(R1A)-LF (Figure 4C), confirming that minTBP-1's ability to mediate both binding and mineralization is critical for the BioLBL process.

Fabrication of Nanodot-Containing Multilayers. The BioLBL procedure also enabled us to accumulate different molecular layers sandwiched between layers of silica. For instance, we prepared three types of minT1-LFs containing different inorganic materials within their respective inner spaces: Fe@minT1-LF contained oxidized Fe, like natural ferritin, while Co@minT1-LF and CdSe@minT1-LF contained oxidized Co and CdSe, respectively. Using these three minT1-LFs, we fabricated two different multilayer structures, in which Fe@minT1-LF, CdSe@minT1-LF, and Co@minT1-LF were stacked in that order or, alternatively, they were stacked in the order Fe@minT1-LF, Co@minT1-LF, and CdSe@minT1-LF. We also fabricated the multilayer that contained three Fe@minT1-LF layers. The QCM signal indicated that the expected layers were formed with these metal-filled ferritins by alternately applying silica precursors and ferritin solution (Figure 5A and B). After three ferritin layers sandwiched by silica layers were deposited, thin cross-sections of the structures were prepared by ion-milling and observed using TEM. Although disturbances most likely due to the cross-sectioning process were apparent, the micrograms clearly showed three layers of ferritin molecules whose thickness was approximately 30 nm (Figure 5C), and EDS mapping further confirmed that, as expected, three types of ferritin were layered (Figure 5D and E). Thus, by using the BioLBL method, we were able to fabricate heterogeneous multilayer nanostructures in a programmable manner.

Conclusions

In this study, we fused minTBP-1 with the L-subunit of ferritin to convey the binding and mineralization capabilities of the peptide aptamer to the cage protein. Alternative application of these two capabilities enabled construction of multiple layers of ferritin separated by intervening layers of silica. TEM revealed the silica layers to be very thin and to apparently act like the mortar between bricks, stabilizing the lamellar structure (Figure 5C). Using this method, we were able to fabricate structures made up of distinct ferritin layers, each containing different nanodots of metal compounds. By fusing the aptamer with other cage proteins having inner spaces of differing size (e.g., 4 nm for *Listeria innocua* ferritin-like protein[29] and 18

nm for cowpea chlorotic mottle virus[14]), it should be possible to fabricate stacks of nanolayers composed of arrays of nanocrystals of distinct size on various substrates. Furthermore, other proteinous biomolecules (antibodies, receptors, etc.) as well as polymer micelles containing inorganic materials[30] could be endowed with binding and mineralization capabilities and incorporated into exquisite architectures fabricated using BioLBL (Figure 6). The current experiments only harnessed TBP-1's capacity for silicification; however, other peptide aptamers also reportedly show a capacity for biomimetic mineralization including ZnS[6] and CoPt,[31] among others.[7,8,32,33] By combining different aptamers, we should be able to expand our repertoire of substances used to compose the layers. The ability to fabricate heterogeneous multilayer nanostructures layers could enable the development of novel types of multi-valued memory elements, battery cells, biosensors, etc.

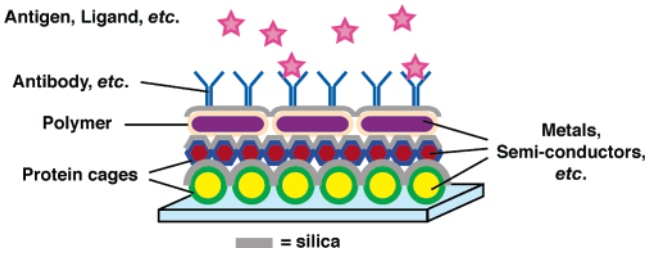

Figure 6. Schematic illustration of hetero-multilayered BioLBL ultrathin film.

Acknowledgment. We thank A. Yamamoto and M. Sugiyama for assistance, and I. Yamashita and K. Iwahori for discussions.

JA057262R

(29) Allen, M.; Willits, D.; Young, M.; Douglas, T. *Inorg. Chem.* **2003**, *42*, 6300−6305.
(30) Ruzette, A. V.; Leibler, L. *Nat. Mater.* **2005**, *4*, 19−31.
(31) Mao, C.; Solis, D. J.; Reiss, B. D.; Kottmann, S. T.; Sweeney, R. Y.; Hayhurst, A.; Georgiou, G.; Iverson, B.; Belcher, A. M. *Science* **2004**, *303*, 213−217.
(32) Brown, S.; Sarikaya, M.; Johnson, E. *J. Mol. Biol.* **2000**, *299*, 725−735.
(33) Yu, L.; Banerjee, I. A.; Matsui, H. *J. Am. Chem. Soc.* **2003**, *125*, 14837−14840.